

Area V5 of the Human Brain: Evidence from a Combined Study Using Positron Emission Tomography and Magnetic Resonance Imaging

In pursuing our work on the organization of human visual cortex, we wanted to specify more accurately the position of the visual motion area (area V5) in relation to the sulcal and gyral pattern of the cerebral cortex. We also wanted to determine the intersubject variation of area V5 in terms of position and extent of blood flow change in it, in response to the same task. We therefore used positron emission tomography (PET) to determine the foci of relative cerebral blood flow increases produced when subjects viewed a moving checkerboard pattern, compared to viewing the same pattern when it was stationary. We coregistered the PET images from each subject with images of the same brain obtained by magnetic resonance imaging, thus relating the position of V5 in all 24 hemispheres examined to the individual gyral configuration of the same brains. This approach also enabled us to examine the extent to which results obtained by pooling the PET data from a small group of individuals (e.g., six), chosen at random, would be representative of a much larger sample in determining the mean location of V5 after transformation into Talairach coordinates.

After stereotaxic transformation of each individual brain, we found that the position of area V5 can vary by as much as 27 mm in the left hemisphere and 18 mm in the right for the pixel with the highest significance for blood flow change. There is also an intersubject variability in blood flow change within it in response to the same visual task. V5 nevertheless bears a consistent relationship, within each brain, to the sulcal pattern of the occipital lobe. It is situated ventrolaterally, just posterior to the meeting point of the ascending limb of the inferior temporal sulcus and the lateral occipital sulcus. In position it corresponds almost precisely with Fischl's Field 16, one of the areas that he found to be myelinated at birth.

J. D. G. Watson,^{1,2} R. Myers,² R. S. J. Frackowiak,² J. V. Hajnal,³ R. P. Woods,⁴ J. C. Mazziotta,⁴ S. Shipp,¹ and S. Zeki¹

¹ Department of Anatomy, University College London, London WC1E 6BT, United Kingdom,

² MRC Cyclotron Unit, Hammersmith Hospital, London W12 0HS, United Kingdom, ³ GEC-Marconi Ltd., Hirst Research Centre, Wembley HA9 7PP and the NMR Unit, Hammersmith Hospital, London W12 0HS, United Kingdom, and ⁴ Division of Nuclear Medicine, Department of Radiological Sciences and Department of Neurology, UCLA School of Medicine, Los Angeles, California 90024

In a previous study, we identified the positions of areas V4 and V5 of human visual cortex, using the technique of positron emission tomography (PET) and relatively simple visual stimuli that emphasized color or motion, respectively (Zeki et al., 1991). In extending our work on area V5, we used new and different motion paradigms in other groups of subjects, only to notice a certain degree of variability in the position of that area outside the V1/V2 complex on the occipitotemporal border that was activated and that we presumed to be area V5. It is conceivable that the new motion paradigms we used, being slightly different from the one we had used originally to identify the position of area V5, might have activated other areas contiguous to V5, and not V5 itself since, in the monkey at least, V5 is known to be surrounded by satellite areas whose cells are also responsive to visual motion though in a more complex way (Zeki, 1980; Desimone and Ungerleider, 1986; Tanaka et al., 1986; Wurtz et al., 1990). On the other hand, it was equally plausible that the position of area V5 itself may not be constant from one individual to the next. This seemed likely, especially in view of the fact that the calcarine sulcus, which constitutes one of the most distinctive landmarks of the human brain, is also markedly variable in position (see Talairach et al., 1967, p 211; Belliveau et al., 1991). Such variabilities raise important questions, especially when imaging studies concentrate on single subjects, as in conditions of disease. We therefore undertook the present studies with two main aims in mind. One was related to the intersubject variability in the position of area V5 and the level of blood flow changes in it in response to the same task. With sufficient numbers of subjects, such a study also affords a comparison of results between subgroups, or between individuals and a group. The latter is not trivial since there are many disease conditions in which the number of subjects available is necessarily limited. Thus, implicit in our approach was our second aim, which was to determine the extent to which conclusions reached by studying single subjects would be representative of those obtained by studying groups.

The above aims naturally made it important to obtain a more accurate picture of the position and relative blood flow increase of area V5 in each individual, by repeating our previous paradigm on a larger num-

ber of subjects and with an improved PET camera, of increased sensitivity. However, even improved PET scans would have been insufficient to solve one of our major problems, and indeed a major problem of cerebral cartographic studies, which is to relate the position of a functionally defined cortical area, in our case area V5, to the sulcal and gyral anatomy of the brain, since PET images are low in spatial resolution and do not highlight such cerebral landmarks. We thus set out to coregister our PET images with images of the same brain obtained with magnetic resonance imaging (MRI), the latter technique being of far greater value in revealing the details of cortical anatomy. Coregistration methods (Pelizzari et al., 1989; Evans et al., 1991) have been described and used to reveal the position of regions that are usually otherwise well defined, such as primary sensory or motor cortex (Grafton et al., 1992). We wanted to go beyond and ask whether a functionally defined cortical area lying well outside the primary visual cortex (V1), in what used to be known as visual "association" cortex, would also have a consistent relationship to the anatomy of the cortex, just as area V1 has a definite relationship to the calcarine sulcus. Coregistering our PET images, obtained from repeated PET measurements within individual subjects, with very high-resolution MR images obtained from the same subjects allowed us not only to examine the variation in sulcal and gyral anatomy in the area of interest, but also to relate this variability to the position of area V5 as defined by PET results.

Materials and Methods

We studied 14 normal volunteers and collected technically satisfactory data from 12 subjects and therefore 24 hemispheres. The results from these 12 are reported here. Of the 12, nine were male and three female; their ages ranged from 21 to 70 years (mean, 43 ± 17 years). Two wrote with the left hand. The degree of hand preference was scored with a short questionnaire based on the Edinburgh MRC handedness scale (Oldfield, 1971; Schachter et al., 1987). The scale ranges from -100, indicating complete left dominance, to +100, for complete right dominance. The two left-handers scored -65 and 0, one right-hander scored 55, while the remaining nine scored 80 or above.

All subjects gave informed written consent. The studies were approved by the Hammersmith Hospital Medical Ethics Committee, and permission to administer radioactivity was obtained from the Administration of Radioactive Substances Advisory Committee of the Department of Health, UK.

Experimental Design

All subjects underwent 12 sequential scans over the course of a single 3 hr session, each scan providing measurements of relative regional cerebral blood flow (rCBF). Changes in rCBF were used as an index of the local synaptic activity elicited by the presentation of specific visual stimuli (Raichle, 1987). The rCBF was compared in two states of stimulation, using the following stimuli.

Stimulus A

Subjects' eyes were open, with the subject viewing a high-resolution Amiga monitor (Commodore Business Machines Inc., West Chester, PA), at a distance of 37 cm. The screen was rectangular and at this distance the display covered the central 30° of the visual field vertically and 40° horizontally. The display consisted of a stationary, random, array of approximately 600 small black squares each subtending 1°, displayed on a white background.

Stimulus B

Subjects' eyes were open, with the same display moving coherently in one of eight directions that changed randomly every 5 sec in 45° steps from 0° to 315°. The small squares moved en bloc at a speed of 6.2 squares/sec in the horizontal and vertical directions, and 5.8 squares/sec in the diagonal directions. The choice of the moving stimulus was derived from our experience with the physiology of area V5 in the macaque monkey, which is characterized by a heavy concentration of direction-selective cells, most of which respond optimally to small spots or squares moving in the appropriate direction (Zeki, 1974). In particular, we arranged that the stimulus motion should be in different directions so as to stimulate as many of the directionally selective cells in V5 as possible. All moving stimuli were translated by one pixel per frame (at a 50 Hz screen refresh rate), which was the smoothest motion that could be generated with our raster-based display unit.

When the display was stationary subjects were asked to fixate a nominated small square at the center of the screen. For the moving display, the subjects fixated a small stationary square at the center. The two stimuli were alternated from scan to scan and, to avoid any possible order effects, the series commenced with one stimulus in half the subjects and with the other stimulus in the other half. Both stimuli were identical in terms of brightness and contrast; the latter was well above 90% and as such would have been expected to stimulate both the magno- and parvocellular systems (Kaplan and Shapley, 1982; Tootell et al., 1988).

Data Acquisition

rCBF was measured by recording the distribution of cerebral radioactivity following the intravenous injection of the freely diffusible positron-emitting ^{15}O -labeled tracer H_2^{15}O . Any increase in rCBF entails an increase in the amount of radioactivity recorded from that region (Mazziotta et al., 1985; Fox and Mintun, 1989).

The measurement of local radioactivity was carried out by scanning the brain with a CTI 953B PET scanner (CTI Inc., Knoxville, TN). The inter-detector collimating septa, which are used conventionally to limit the detection of scattered radiation, were removed to increase the acceptance angle and hence the number of photons recorded. The inevitable increase in noise due to scattered photons is more than adequately compensated for by the more efficient use of the administered radioactivity (Townsend et al., 1991). Spe-

specifically, the point source sensitivity is six to seven times higher than with a standard machine like the CTI 931 scanner recording with the septa in place (Bailey et al., 1991a). In practice, there is a threefold increase in useful counts over the whole brain and a fivefold increase at the center of the field of view (Bailey et al., 1991b). An advantage of this is that less radiation need be administered per scan and therefore more scans can be performed in each subject. The averaging of more scans with each stimulus results in improved signal to noise, producing data of a quality sufficient for the identification of activated regions in the brains of individual subjects, and is clearly an improvement of substance in the study of individual patients. To date, the sensitivity of conventional PET scanning has been such that meaningful data could not usually be obtained from single subjects, especially if the changes in rCBF were not large, and this necessitated the averaging of activations from groups of subjects. Here we show that with our more sensitive technique, we can obtain reliable data from single subjects.

The scanner collects data from 16 rings of crystal detectors covering an axial field of view of 10.65 cm. The emission data were corrected for the attenuating effects of the tissues of the head by using measurements made from a transmission scan collected prior to the activations. The corrected emission data were then reconstructed as 31 axial planes by filtered back projection with a Hanning filter of cutoff frequency 0.5 cycles/pixel. The resolution of the resulting images was $8.5 \times 8.5 \times 4.3$ mm at full-width half-maximum (FWHM) (Spinks et al., 1992). Each plane was displayed in a 128×128 pixel format, with a pixel size of 2.0×2.0 mm. The 31 original planes were transformed by interpolation to 43 planes, to produce images with approximately cubic voxels.

Each rCBF measurement began with a background scan lasting 1 min. Ten seconds prior to the end of this scan, the subjects opened their eyes and started to view the computer display. A second 3 min scan started immediately after the background scan, and at its beginning an $H_2^{15}O$ infusion was started. The infusion was at 10 ml/min and continued for 2 min, and was followed by a 30 sec flush of nonradioactive normal saline. This procedure differs from our previous technique of generating circulating $H_2^{15}O$ in which subjects inhaled $C^{15}O_2$ (Zeki et al., 1991). The process was repeated 12 times in each subject with 12 min between scans to allow for the decay of radioactivity to background levels. The integrated counts accumulated over the 3 min of the second scan, corrected for background activity (first scan), were used as an index of rCBF. On average, each subject received 1014 MBq of $H_2^{15}O$ for each of the 12 scans.

Image Transformations

All calculations and image manipulations were carried out on Sun 3/60 and SPARC computers (Sun Computers Europe Inc., Surrey, UK), using ANALYZE version 5 image display software (BRU, Mayo Foundation, Rochester, MN) and PROMATLAB (MathWorks

Inc., Natick, MA). Statistical maps of significant blood flow change were then derived using SPM software (MRC Cyclotron Unit, London, UK). The PET scans were analyzed in three ways: as a group in transformed (Talairach) coordinates, as individuals in the same space, and as individuals untransformed, in their own anatomical space defined by MR imaging. Figure 1 sets out the steps in image manipulation and analysis, in diagrammatic form.

Anatomical Standardization

In all three analyses the first step was to correct for head movement between scans by aligning them all with the first one, using Automated Image Registration (AIR) software specifically developed for the purpose (Woods et al., 1992). To analyze the results obtained from groups of subjects the 12 realigned images from each subject were averaged and the intercommissural (AC-PC) line, linking the anterior to the posterior commissure, identified. All the images from all subjects were then transformed into the standard anatomical space of the stereotaxic atlas of Talairach and Tournoux (1988), which uses this line as its reference point. This transformation was done by using linear proportions and nonlinear resampling algorithms (Friston et al., 1991a) using some additional information derived from MRI scans. In this stereotaxic space each pixel measures 2×2 mm, with an interplane distance of 4 mm. With individual brains an identical procedure was employed for image re-alignment and stereotaxic normalization prior to statistical manipulation on a subject-by-subject basis, rather than as a group. This was undertaken so that the position of activated regions could be reported in Talairach coordinates for comparison between subjects and with previous and future results. For the purposes of PET to MR image coregistration in individuals, no anatomical transformation was undertaken.

Smoothing of PET Images

The PET images (group and individual) were all filtered with a low-pass Gaussian filter (FWHM of $5 \times 5 \times 3$ pixels, $10 \times 10 \times 12$ mm) to smooth the data in three dimensions (Friston et al., 1990). This served to increase the signal-to-noise ratio by attenuating the high-frequency noise in the images, and by augmenting the effects of image averaging across subjects, when performed.

The filter that we used for individual and group analysis was considerably smaller than the filter we had used with the poorer-resolution and lower-sensitivity PET camera in previous group studies (Zeki et al., 1991). The better resolution and sensitivity of the PET camera used in this study improved signal-to-noise characteristics sufficiently to permit the use of a smaller filter with equal effect.

Statistical Analysis

We used the technique of statistical parametric mapping (SPM) for data analysis (Friston and Frackowiak, 1991).

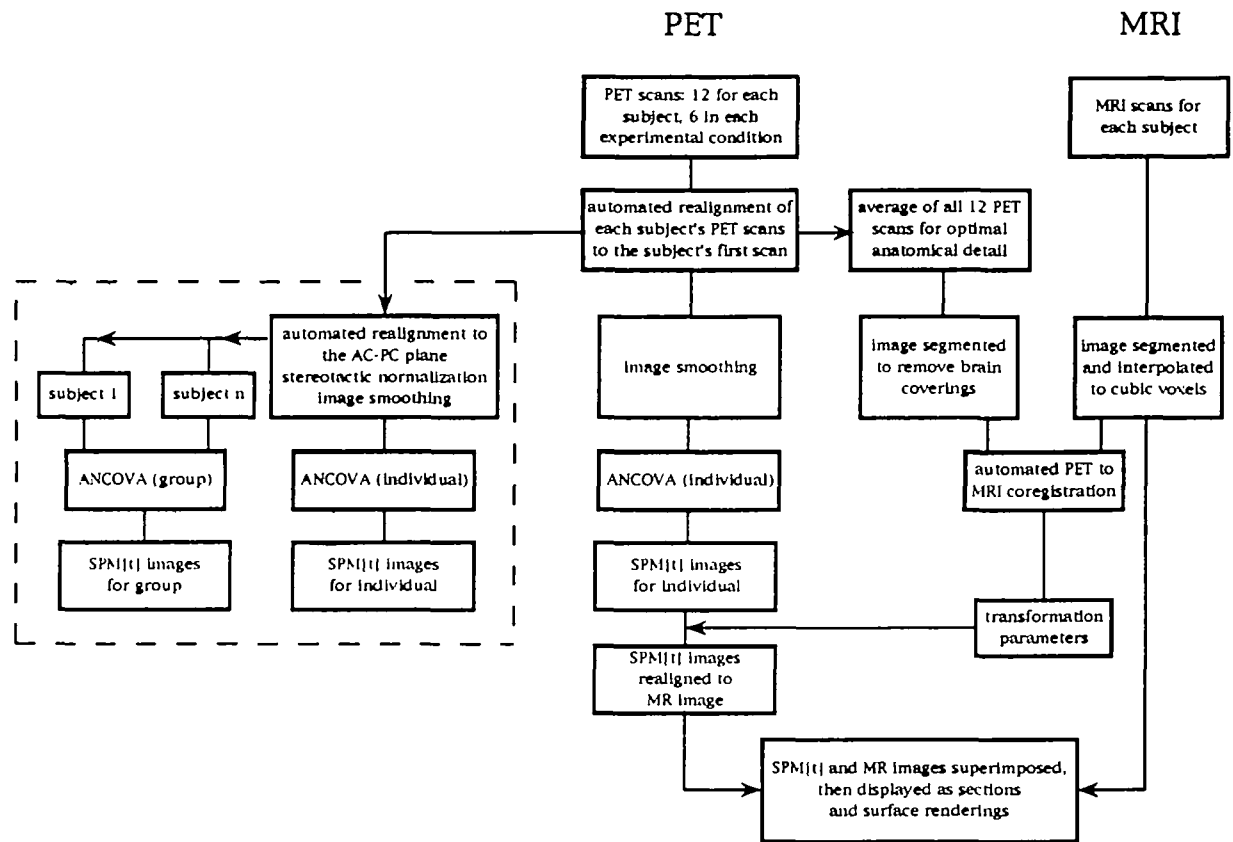


Figure 1. Flow diagram illustrating the stages of data acquisition, image manipulation, and statistical analysis used in this series of experiments. Note that on the left, inside the broken outline, all the images have been transformed into the stereotaxic coordinate system of Talairach and Tournoux (1988). On the right, the PET and MRI images were not thus transformed.

For Groups

When activation leads to a change in rCBF, the change may be confounded by differences in global flow between subjects, or within each subject between scans. We corrected for this confounding effect by performing a pixel-based analysis of the covariance (ANCOVA) of rCBF against relative global CBF, the latter being treated as the confounding covariate (Friston et al., 1990). The ANCOVA is used to calculate, for each pixel, the mean values of rCBF across subjects (with the global CBF adjusted to 50 ml/dl/min), together with the associated error variance. This is performed separately for each of the sequence of 12 scans by pooling the data for each comparable scan across all subjects.

To compare the activity elicited in the brain by the static and moving stimuli, the difference between the six mean values of rCBF obtained for each of the two visual conditions was evaluated, again for each pixel, by use of the t statistic, transformed to the normal distribution. This generated a statistical parametric map ($SPM\{t\}$) of the areas of significant rCBF change associated with the difference in the tasks. On such an $SPM\{t\}$, only pixels whose significance values exceeded a certain threshold were displayed. The level of the threshold is set to correct for the effective number of independent tests constituting the SPM , which is less than the actual number of pixels because neighboring pixels are not truly independent (the theory and practical aspects of setting the statistical thresh-

olds are to be found in Friston et al., 1991b). Pixels exceeding threshold were then displayed on coronal, sagittal, and transverse views of the brain as projection maps. The stereotaxic coordinates of the most significant sites of change were determined and correlations with anatomical areas made by reference to the standard atlas (Talairach and Tournoux, 1988).

The pixels with maximally significant stimulus-related activation were used to estimate the relative size of the changes in rCBF. These values represent adjusted, average rCBF from spherical regions of approximately 10 mm in diameter centered on the chosen coordinates.

For Individuals

A procedure similar to the one described above was used for analyzing the pattern of rCBF change in individual subjects. The $SPM\{t\}$ was noisier than for the group analysis (six scans from the same individual were averaged and compared with six others, as opposed to 72 scans from 12 subjects compared against 72). Hence, a secondary Gaussian smoothing filter of 4 mm FWHM was applied to the $SPM\{t\}$ in the x- and y-dimensions. The effect of this filter was a small change in the in-plane resolution, on average from 9.9 mm FWHM to 10.7 mm.

The average location of significant areas of change obtained from the group analysis of the 12 subjects was used to direct the search for the location of area V5, that is, for a bilateral prestriate area in the an-

terolateral parts of the occipital lobe in which cortical activation by visual motion might be expected in each individual. We were interested in this part of the occipital lobe because (1) our previous work had suggested that the zone of maximal rCBF change with a motion stimulus would occur here (Zeki et al., 1991); (2) the evidence from a study of the patterns of callosal connectivity and myelination in the human brain, and its relation to the same pattern in the monkey brain, suggested this region as the most plausible site (Clarke and Miklossy, 1990); and (3) this is the general region implicated in cerebral akinetopsia (Zihl et al., 1983, 1991), even if the lesion in that patient was relatively large.

In more precise terms, we first identified the position of area V5 in the group of 12 brains, by determining the region of maximal rCBF change in this part of the occipital lobe. With V5 so defined, we next defined the distance of the search radius, that is, the regions from the center of V5 that we were prepared to consider as belonging to V5 in any given individual, which we set at 15 mm, that is, 1.5 times the FWHM of the primary smoothing filter. This search distance is arbitrary: we felt that it should be larger than the primary smoothing filter, as a narrow search based on the location of V5 determined by image averaging across all subjects would by definition exclude an individual site of V5 that was far enough away from the mean to contribute little or nothing to that mean position. On the other hand, too large a distance would lead to the inclusion of areas such as the V1/V2 complex that we would not consider as candidates for the location of V5 in individuals. Finally, we accepted an activation as significant and as belonging to V5 if it occurred on at least three contiguous axial planes.

Thus, by limiting the number of pixels interrogated, we could afford to use less stringent statistical thresholding. Thresholding of the SPM{ t } was carried out with decreasing degrees of harshness, in arbitrary steps determined by the SPM software, starting with $p < 0.05$, corrected for multiple nonindependent comparisons (a Z score of about 3.8). The threshold was then lowered to $p < 0.001$, without a correction for multiple comparisons (a Z score of 3.09), if no significant activation could be found, and finally to a threshold of $p < 0.01$ (a Z score of 2.33) until an activation could be found in the searched region. The location of the pixel with the most significant Z score was taken to be V5. Because the primary filtering was carried out in all three dimensions, the coordinates of this point lay close to the center of the area of significant change within the appropriate plane, and this plane was at or near the center of the contiguous planes when considered in the z-dimension. In other words, this point lay at or very close to the center of mass of each V5.

PET-MRI Coregistration

For the coregistration of SPM and MR images obtained from individual brains, the steps of image realignment to the intercommissural line and anatomical standardization were omitted. However, the subsequent

filtering, followed by ANCOVA and the generation of a thresholded SPM{ t }, were identical. For each individual, the SPM{ t } was then coregistered with the subject's own MRI scan. Such superimposition allowed us to determine the position of the region of maximal rCBF change in relation to the gyral and sulcal pattern of that brain, with the hope of learning whether there is any consistent relationship between the two.

The MRI scans were obtained with a 1 tesla Picker HPQ Vista system using a radiofrequency (RF) spoiled volume acquisition that is relatively spin-lattice relaxation time (T1) weighted to give good gray/white contrast and anatomical resolution [repeat time (TR) 24 msec; echo time (TE) 6 msec; nonselective excitation with a flip angle of 35°; field of view in plane 25 × 25 cm; 192 × 256 in plane matrix with 128 secondary phase-encoding steps oversampled to 256; resolution 1.3 × 1.3 × 1.5 mm; total imaging time 20 min]. After reconstruction, the MR images were also aligned parallel with the intercommissural line, and interpolated to yield a cubic voxel size of 0.977 × 0.977 × 0.977 mm, which permitted coregistration with the PET images.

A PET image with the best possible anatomical detail was constructed by averaging the 12 realigned PET scans from each individual. A rigid body coregistration with the MRI scan was carried out using the AIR software originally developed for PET to PET realignment with adaptations for this purpose (Woods et al., 1992). In separate validation studies, the mean error in the alignment of the two images was approximately 1 mm, with a maximum error of 2 mm (R. P. Woods, unpublished observations). The reorientation parameters in terms of translations in x, y, and z and rotations about these axes were calculated. These parameters were saved and used subsequently to coregister the statistical parametric maps of significant rCBF change (which contain little anatomical information) with the subject's cerebral anatomy as described by the MRI scan.

Results

We describe under separate headings the results obtained from the entire group of 12 subjects analyzed as a single group, from selected subgroups of six subjects and from individual subjects analyzed as individuals. Implicit in this subdivision is one of the main aims of this work, namely, the extent to which results obtained from small groups or single individuals, in terms of location of a functional area and the extent of blood flow change in it, are valid for a larger population of brains.

Group Results

V5: The Motion Areas

Our first step was to confirm that there is an area situated on each lateral occipital surface associated with the perception of visual motion. We have indeed been able to do this: Figure 2 and Table 1 document the highly significant foci of increased rCBF induced

Table 1

Cortical areas associated with the perception of visual motion: grouped data from 12 subjects comparing visual motion with a static visual image

Region	rCBF (adjusted group means; ml/dl/min)		Talairach coordinates	Z score
	Static	Motion		
Left V5	54.8	57.4	-44, -70, 0	7.83
Right V5	52.3	54.8	+40, -68, 0	9.05
Mean	53.6	56.1		
V1/V2	73.3	78.0	+2, -88, 0	11.03
	68.4	72.6	+4, -88, +4	11.03
Mean	70.9	75.3		

The points recorded are those with the highest Z scores within each area. The two points given for V1/V2 share the same Z score of 11.03, the highest significance value that could be accommodated by the SPM program. The coordinates for V5 may be compared with the group data from the previously reported three subjects, that, when reanalyzed in the same fashion as the present experiment, gave locations for V5 of -46, -62, +8 on the left and +42, -66, -4 on the right (Zeki et al., 1991).

in our subjects by looking at the dynamic rather than static visual display. As before, we conclude that this represents the motion area V5 in man. The average increase in rCBF in a 10 mm diameter spherical region of interest centered on the pixels of most highly significant change was 4.7%. The anatomical coordinates of the points of maximally significant change are comparable to those obtained from an earlier group of three subjects studied on a different PET scanner (Zeki et al., 1991). The present results are more accurate because we have since been able to identify the position of the AC-PC line more accurately using the coregistration of PET and MR images. This has resulted in an anatomically more reliable transformation into stereotaxic space. In fact, when we used the improved stereotaxic transformation obtained from the present results to reanalyze the stereotaxic position of area V5 obtained from our earlier group of three, the position of V5 in the two studies is quite similar (see Table 1). The average blood flow change was less in the study of the present group compared to the earlier and smaller group of three (4.7% vs 6.1%).

As previously, our results expressed in Talairach and Tournoux coordinates show that human area V5

has a ventrolateral location, at the confluence of the occipital and temporal lobes, and at the junction of Brodmann's areas 19 and 37 inferiorly.

Other Areas

In addition to the activation in V1 and V2 (see Table 1; the difficulty of separating the two areas is discussed in Zeki et al., 1991), the improved resolution and statistical power of the present experiments revealed separate areas of activation, not seen in our previous study (see Figs. 2, 4). One zone of activation lies in the cuneus and extends laterally onto the surface of the brain superiorly. It may correspond to parts of areas V3 and V3A identified in the monkey by a combination of anatomical and physiological criteria (Cragg, 1969; Zeki, 1969, 1978). This is a topic that we shall address in a subsequent report.

Subgroup Analysis

Our experiment with 12 subjects provided seventy-two measurements in each of the two states, and thus represents a comparatively large sample size. Most studies use smaller groups. This made it interesting to ask how representative results obtained from smaller groups would be. One way of approaching the issue was to take different samples of six subjects from the whole group and contrast the location and extent of rCBF changes of human area V5 in them.

There are 924 possible combinations of 6 from 12. It was not practicable to test all of these with our current software. Various subgroups of six were therefore chosen in such a way as to maximize the potential variability in position and blood flow change of V5, to obtain information about limiting cases. For example, a subgroup of six individuals was chosen in which left V5 was more anteriorly placed; hence, the complementary subgroup of the remaining six subjects had more posterior locations for left V5. Other subgroups of six were chosen with the aim of maximizing or minimizing the rCBF increases for V5. The results are given in Table 2, which shows that between two groups of six subjects, drawn from a population of 12, the position of the most significant pixel of V5 in stereotaxic coordinates may vary, in the limiting case, by as much as 13 mm. Group blood flow in-

Table 2

Subgroup analysis: variation in the location of the most significant pixel of V5 and the rCBF increases at this point for selected samples of six subjects

Group	Individual feature	Talairach coordinates	rCBF (adjusted group means; ml/dl/min)		Relative rCBF increase (%)	Z score
			Static	Motion		
1	Left V5, more posterior	-40, -72, -4	55.9	58.2	4.2	5.88
2	Left V5, more anterior	-44, -62, +4	54.6	57.9	6.0	6.83
3	Right V5, more inferomedial	+40, -64, 0	52.9	55.3	4.5	7.33
4	Right V5, more superolateral	+48, -66, +4	45.7	48.1	5.1	6.42
5	Left V5, greater rCBF increases	-42, -66, 0	54.6	58.0	6.3	6.13
6	Left V5, less rCBF increases	-46, -62, +4	56.5	58.4	3.4	5.56
7	Right V5, greater rCBF increases	+38, -66, 0	51.6	54.9	6.3	7.81
8	Right V5, less rCBF increases	+38, -60, 0	49.3	51.1	3.7	6.23

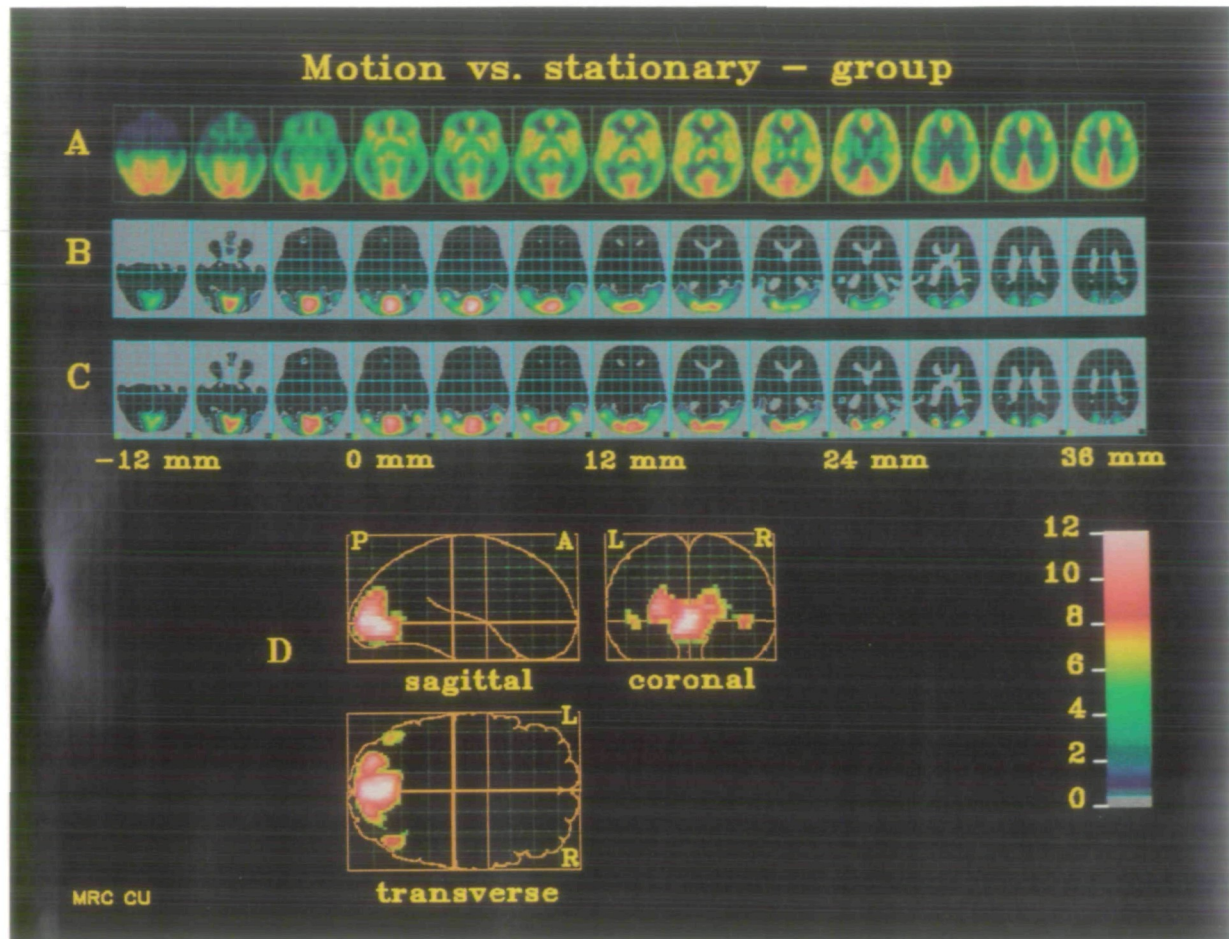


Figure 2. Data averaged from the entire group of 12 subjects. At the top are transverse images of the brain after stereotaxic normalization, with the distances from the AC-PC plane indicated. *A*, Anatomical features obtained by averaging all blood flow scans from all subjects. *B*, The arithmetical difference between adjusted mean blood flows for moving and stationary stimuli. *C*, The $SPM\{t\}$ values derived from the formal pixel-by-pixel comparison of the adjusted mean blood flows and variances for each of the two conditions. The color scale on the right applies only to row *C* and reflects the Z value of each pixel in the $SPM\{t\}$ images. *D*, The orthogonal projections of the statistical comparison at a threshold of $p < 0.00001$, corrected for multiple comparisons (a mean Z value of 6.1). The areas showing significant increases in blood flow are on the lateral occipital surfaces at the junction of areas 19 and 37 of Brodmann (V5), the V1/V2 complex, and an area arising in the cuneus on each side and extending superiorly.

creases recorded in response to a moving stimulus might range from 3.4% to 6.3%.

Individual Results

We wanted to extend our studies to single subjects, since information obtained from a single subject may be crucial, especially in cases of disease where the number of subjects may be very limited. For example, to date only one good example of cerebral akinetopsia has been described (Zihl et al., 1983, 1991).

Position of Area V5

In the left hemisphere, the position of the most significant pixel corresponding to V5 in Talairach space varied more than on the right (Fig. 3, Table 3). The range was 27 mm on the left and 18 mm on the right. We could discern no relationship between the individual locations and age, sex, or handedness score.

Blood Flow Changes in V5

There was an average rCBF increase of 3.9 ml/dl/min in the left V5 areas associated with the perception of

visual motion (range, 1.4–5.4 ml/dl/min). In the right hemisphere, the mean increase was 3.7 ml/dl/min (range, 2.3–5.7 ml/dl/min). In relative terms, the mean increases were 7.1% on the left (range, 2.6–9.6%) and 7.2% on the right (range, 4.2–11.5%). No relationship was found between blood flow changes and age, sex, or handedness. The higher individual blood flow increases were associated with greater statistical significance.

Seventeen of the 24 V5 areas were significant at the harshest threshold of $p < 0.05$ (corrected for multiple comparisons), with Z scores from 3.86 to as high as 8.52. Six areas were significant in the next lower range, with Z scores of 3.09–3.66. In only one case was the threshold lowered further in order to discern area V5 (a threshold of $0.001 < p < 0.01$, with a Z score of 2.46). As the area of search for V5 was constrained by a knowledge of its location in the averaged group results, even this result may be considered significant. The fact that 17 V5 areas were identified at the threshold of $p < 0.05$ (corrected for multiple comparisons) means that they could have been reported in their own right, with no prior knowledge

Table 3

Locations for the most significant pixel of V5 in the 12 individual subjects, with their associated rCBF increases

Sub- ject	Talairach coordinates	Left V5					Right V5					
		rCBF					rCBF					
		Stat- ic	Mo- tion	In- crease	(%)	Z score	Talairach coordinates	Stat- ic	Mo- tion	In- crease	(%)	
n163	-44, -62, +8	49.3	52.7	3.4	6.9	3.3	+46, -66, 0	51.7	54.9	3.2	6.2	2.5
n164	-38, -66, 0	53.6	55.0	1.4	2.6	3.2	+36, -66, -4	57.3	63.0	5.7	10.0	4.4
n172	-46, -62, +4	56.3	61.7	5.4	9.6	4.2	+46, -64, +4	49.5	53.6	4.1	8.3	4.0
n180	-42, -74, -4	53.7	56.9	3.2	6.0	4.1	+44, -66, 0	52.3	57.1	4.8	9.2	5.7
n185	-36, -72, 0	53.6	56.3	2.7	5.0	3.5	+40, -68, 0	53.5	56.1	2.6	4.9	3.9
n191	-44, -62, +8	56.2	61.1	4.9	8.7	3.9	+40, -78, +4	46.6	49.9	3.3	7.1	4.5
n192	-46, -68, 0	56.0	61.4	5.4	9.6	4.2	+40, -68, 0	49.7	55.4	5.7	11.5	4.3
n197	-46, -70, -4	58.1	61.9	3.8	6.5	4.3	+34, -64, 0	49.6	52.9	3.3	8.7	4.1
n205	-48, -64, 0	57.7	62.0	4.3	7.5	4.5	+42, -60, +4	55.4	59.2	3.8	6.9	5.3
n210	-40, -72, 0	55.4	58.7	3.3	6.0	4.4	+42, -72, +4	42.2	44.7	2.5	5.9	3.1
n216	-30, -82, -4	54.0	59.2	5.2	9.6	8.5	+40, -68, +4	54.4	56.7	2.3	4.2	3.3
n221	-34, -68, 12	47.0	50.2	3.2	6.8	4.2	+38, -62, +8	45.1	47.8	2.7	6.0	3.3
Mean	-41, -69, +2	54.2	58.1	3.9	7.1		+41, -67, +2	50.6	54.3	3.7	7.2	
SE	5.6, 6.0, 5.3	3.3	3.9	1.2	2.1		3.7, 4.7, 3.2	4.4	5.0	1.2	2.1	

The rCBF measurements are expressed in ml/dl/min, adjusted to a mean whole brain blood flow of 50 ml/dl/min for each subject

of their likely positions anywhere in the brain (Friston et al., 1991b).

Area V1/V2

Our confidence in all the above results was reinforced by the control built in to the experiment, namely, the activation of areas V1 and V2, from which V5 receives its input. We have discussed elsewhere the difficulties of separating V1 and V2 in these PET images (Zeki et al., 1991), but we nevertheless expected that in every subject, and in groups of subjects, the activity in V1/V2 must lie along the calcarine sulcus, one of the most conspicuous landmarks in the cerebral cortex and whose position is easily determined from the MR images. The position of the calcarine sulcus is highly variable in individuals, even after normalization to the stereotaxic framework of Talairach and Tournoux (Talairach et al., 1967, p 211; Belliveau et al., 1991). Significant activation was detected in all individual subjects at atlas coordinates consistent with the location of the calcarine sulcus, or along the lingual gyrus beneath it. Coordinate locations alone were not then sufficient to determine the precise anatomical location of this functional activation, but the individual PET/MR coregistrations were able to show that this activation center was truly centered along the course of the calcarine sulcus in all subjects, and thus was felt to represent area V1/V2.

We were also interested to note that, in addition to the rCBF changes in V5 and the cuneus, there were also changes in the parietal lobe, corresponding to Brodmann's area 7 (Fig. 4). This was found in all four subjects for whom the head positioning in the PET camera was such that we were able to scan as high as the vertex.

Coregistration of Individual PET Results with MRI

The coregistration of PET SPM{t} images with the MRI scans obtained from the same brain allowed us

to examine the anatomical location of the activated areas in relation to the sulcal and gyral pattern of the occipital lobe more precisely than had been previously possible. Figure 6 shows surface renderings of both hemispheres from four subjects. The zones of activation were not exclusively superficial, but have been projected onto the surface of each hemisphere in order to illustrate their relation to the overall cortical topography. Figure 5 shows a series of slices through the brain shown in the top row of Figure 6. The bilateral sites of activation corresponding to V5 can be traced through at least five or six slices. Their precise size depends on the level of filtering and statistical thresholding, but each is comparable in extent to the width of a gyrus. The focal points of activation are recessed from the cortical surface. In the right hemisphere, at least, the focus occupies the posterior bank of a relatively deep fissure that, by reference to Figure 6, is seen to be a vertically oriented sulcus, one that might be identified as the posterior continuation of the inferior temporal sulcus. The same may be true for the focus in the left hemisphere, though the judgment is rather more equivocal. As elsewhere in the human cerebrum, the disposition of sulci in the occipital lobe is highly variable and there is a corresponding imprecision in the terminology. We thus postpone to the Discussion the question of a consistency in the relationship of a functionally defined cortical area, V5, which we were able to identify in all 24 hemispheres, to a gyral configuration that is rather less predictable.

Discussion

The group results from 12 subjects revealed areas of the human visual cortex that were differentially and commonly activated by the visual motion stimulus that was used. These included the area that we had previously identified as the human equivalent to monkey V5, V1/V2, and other sites not reported before in

Variation in position of V5

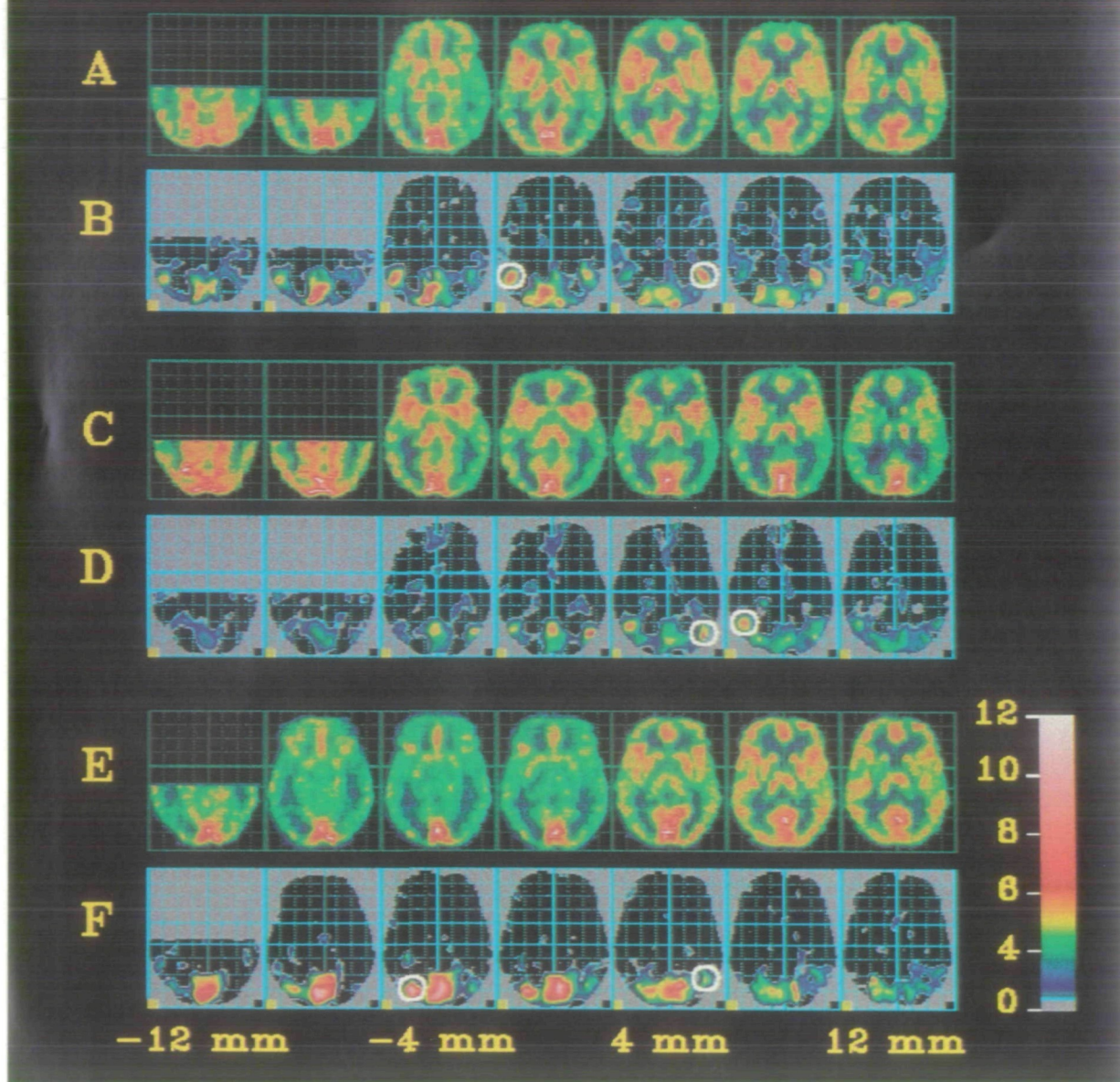


Figure 3. Data from three individual subjects to show the maximum range in the position of V5 on each side, after stereotaxic normalization. *A*, *C*, and *E*, Transverse images of blood flow for each subject to show anatomical detail, obtained by averaging the 12 scans from the subject. Distances from the AC-PC plane are indicated. *B*, *D*, and *F*, SPM{ t } images obtained for each subject. The locations of the most significant pixel for left V5 are, in *B*, $-48, -64, 0$; *D*, $-44, -62, +8$; and *F*, $-30, -82, -4$. For right V5, the locations are $+42, -60, +4$ in *B*, $+40, -78, +4$ in *D*, and $+40, -68, +4$ in *F*. These locations are indicated by the white circles. The distance separating left V5 in *D* and *F* is 27 mm, while the separation between the right V5 of *B* and *D* is 18 mm. The three sets of SPM{ t } images are scaled to the same range of Z values, indicated by the color scale on the right.

terms of a specific motion stimulus, nor yet characterized in terms of homology with monkey occipital and parietal cortex. Second, we were able to find these same regions of significant rCBF change in individuals—particularly in area V5, located bilaterally in the anterolateral part of the occipital lobe. Third, this allowed us to gauge the variability between individuals undertaking the same task, both in the position of area V5 and in the magnitude of its rCBF change. Finally, we used high-resolution MRI scans to determine how far the variable location of V5 could be

ascribed to individual variation in patterns of gyral anatomy, as distinct from inconsistencies in stereotaxic normalization.

The Identification of Area V5

The results reported here, based on a study of 12 subjects and using an improved PET camera with a higher sensitivity, confirm the results we obtained from our previous study (Zeki et al., 1991) of three subjects scanned in an older PET camera (CTI-Siemens 931) (Table 1). The present results allowed us,

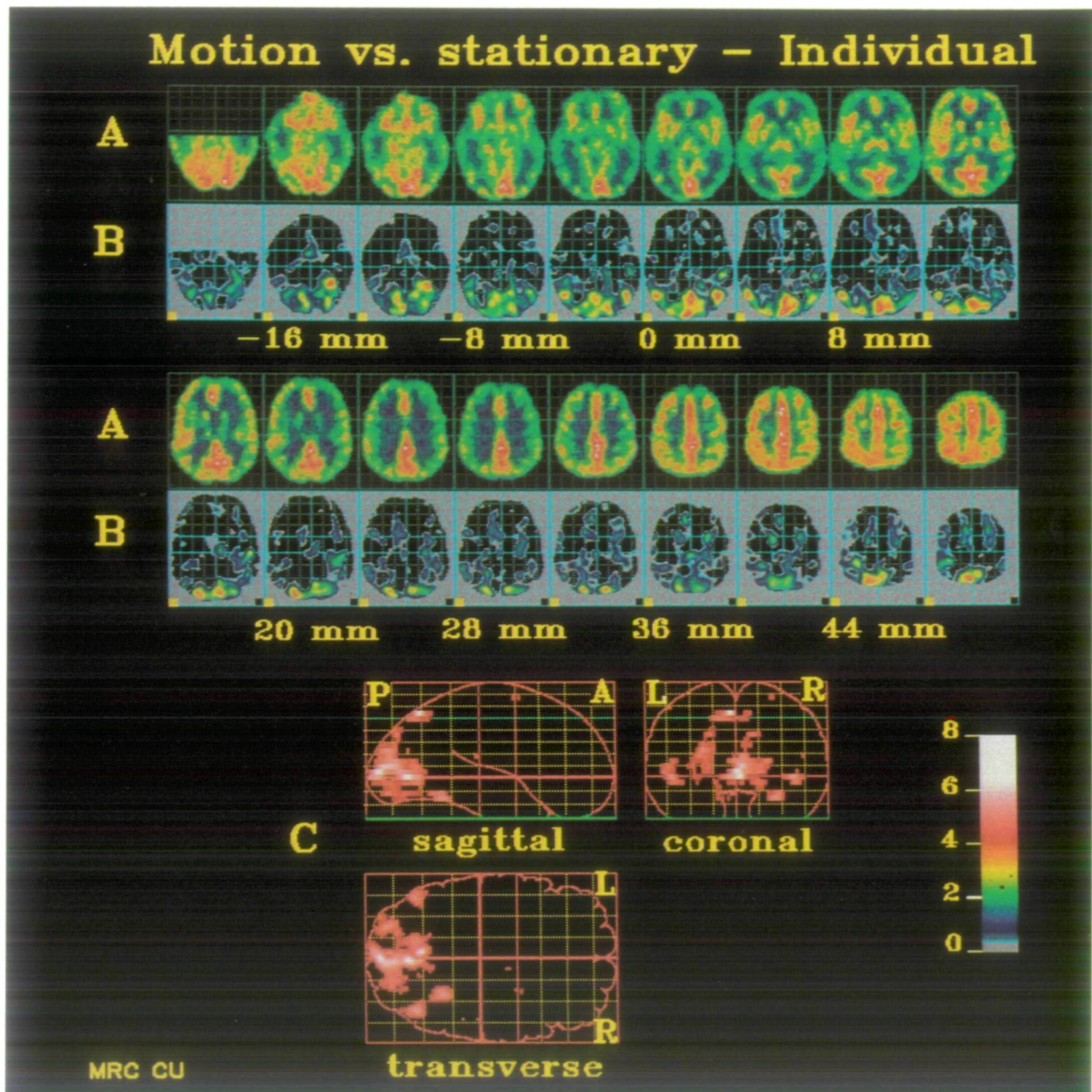


Figure 4. Data from a different single subject to those shown in Figure 3. *A*, The anatomical details on transverse planes parallel with the AC-PC plane obtained by averaging the 12 blood flow scans, after stereotaxic normalization. *B*, The SPM(t) images for this subject. The images share a constant color scale for the Z values in each pixel, indicated on the right. *C*, The orthogonal projections of the SPM(t) at a threshold of $p < 0.001$, uncorrected for multiple comparisons. V5 can be identified on both sides, as can areas of increased blood flow in the V1/V2 complex and both cuneate areas, extending superiorly. Also seen are areas of increased blood flow in the superior parietal lobes, from the border of the occipital lobe forwards, corresponding to Brodmann's area 7.

however, to obtain a clearer picture of the variability in the position of area V5. Moreover, the use of the new camera made it possible to coregister the PET images with the MR images and thus relate the position of area V5 to the sulcal and gyral anatomy of the occipital lobe.

Our previous study, perhaps because of the lower sensitivity of the camera, revealed only one candidate prestriate area that was consistently present when motion was the critical stimulus. In addition to the result itself, there was more than one line of reasoning that suggested that the active area in our previous study must be V5. Its location was closely similar to that indicated by Clarke and Miklossy (1990) from their

anatomical studies. They used two criteria: one related the position of the prestriate areas to the pattern of callosal distribution within that zone of cortex, since cortical areas have a definite relationship to strips of callosally connected cortex (Zeki, 1977a,b), and the other related to the pattern of myelination within the prestriate cortex. These anatomical studies showed that V5 must be located fairly ventrally on the lateral surface of the occipital lobe. It was this very territory that was compromised in the akinetopsic patient described by Zihl et al. (1983, 1991), although the lesions went beyond the confines of the area that we now define as V5. It thus seems more than plausible to suppose that the area we describe here and else-

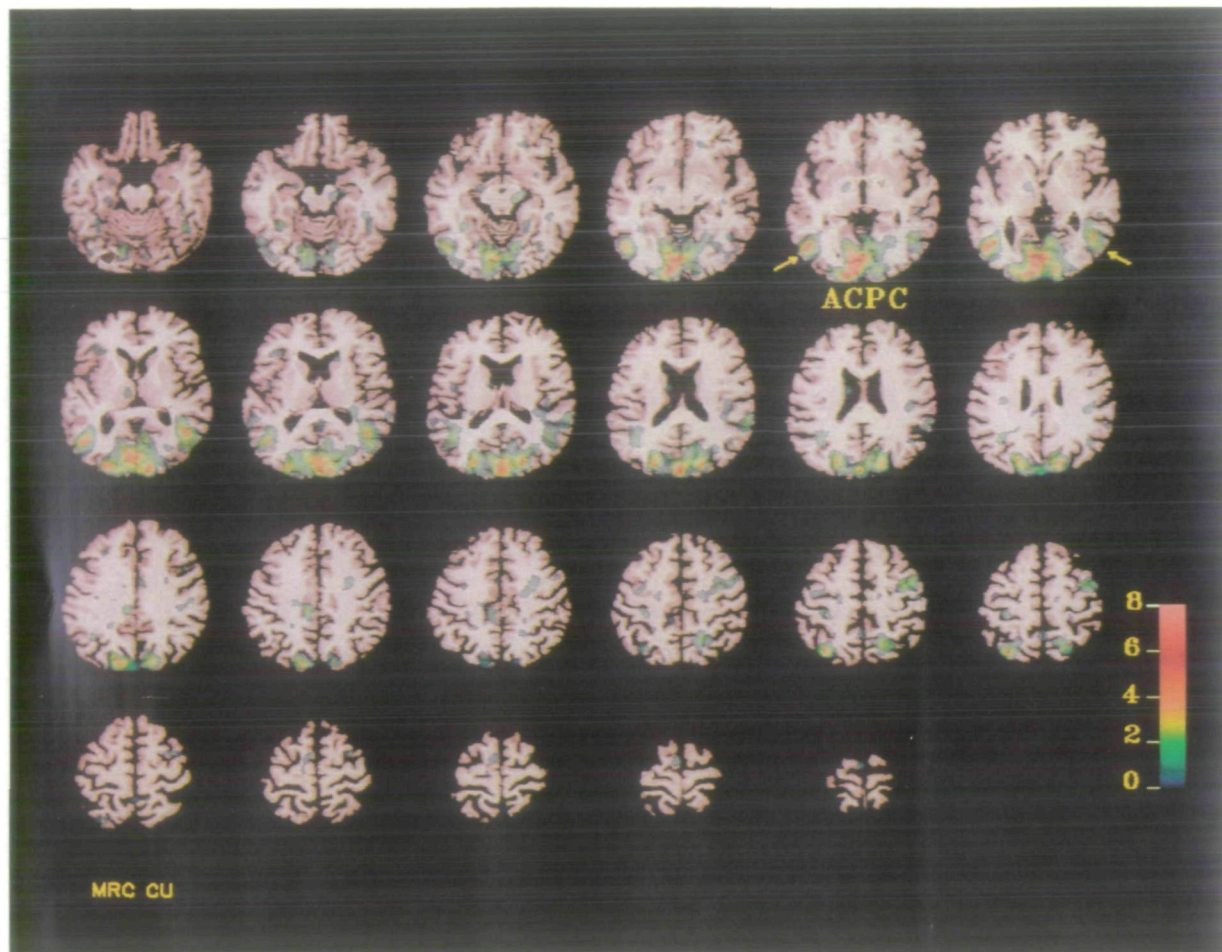


Figure 5. Data from a single subject in which the MR images and SPM{*t*} images have been coregistered and superimposed. Axial slices at 4 mm intervals are depicted, parallel with the AC-PC plane, which is indicated by ACPC underneath the relevant slice. The SPM{*t*} images share a common color scale for their pixels' Z values, indicated on the right. At the AC-PC level there is activation along the calcarine sulcus, reflecting activity in the V1/V2 complex. V5 is present on each side and is indicated by arrows; in particular, the relationship with underlying sulci is seen. On both sides there is also significant activation inferiorly in the lingual gyri and superiorly, arising from the cuneus and continuing upward.

where is human V5. As far as we can tell from the abstract published by Miezin et al. (1987), an area overlapping with the one reported here but extending to the parietal cortex was among the areas identified using a visual motion stimulus.

The Variability in the Position of Area V5 in Individuals

Using the same general strategy of image realignment to the intercommissural plane, followed by stereotaxic normalization, we found that the previously reported study on V5 in three subjects, analyzed in the same way as the present 12 subjects (using the same stereotaxic transformation), would place V5 on the left more anterosuperior to the location here determined, by some 12 mm (Table 1). On the right the difference is only some 5 mm. Our supposition was that such differences might be due to the variation in the precise position of V5 in different individuals, rather than to any systematic difference introduced by the new PET machine. Closer analysis of the results confirms this.

The location of V5 in Talairach coordinates was determined for both hemispheres in each individual

from SPM{*t*} maps, following the same image realignment and stereotaxic normalization used for the group analysis. When the 12 subjects were analyzed as individuals, the extreme variation in position of V5 was 27 mm on the left and 18 mm on the right (Table 3). The analysis of the subgroups of six presented in Table 2 also demonstrates that such selections of subgroups, tested with an identical experimental paradigm, can yield mean locations for V5 that differed from each other by as much as 13 mm.

A similar analysis of variability can be carried out for changes in rCBF. The maximum relative individual increase in rCBF for V5 in the present study was 11.5% and the minimum was 2.6% (Table 3). The average of all the individual values was 7.1% on the left and 7.2% on the right. However, the increases obtained when the 12 subjects were incorporated into a single group prior to analysis were 4.7% on the left and right (Table 1). The analysis of subgroups of six (Table 2) shows that relative increases in blood flow reported for V5 could vary from 3.4% to 6.3% on the left and 3.5% to 5.8% on the right. The rCBF changes derived from the averaged data are smaller than those recorded in individuals because of the combination

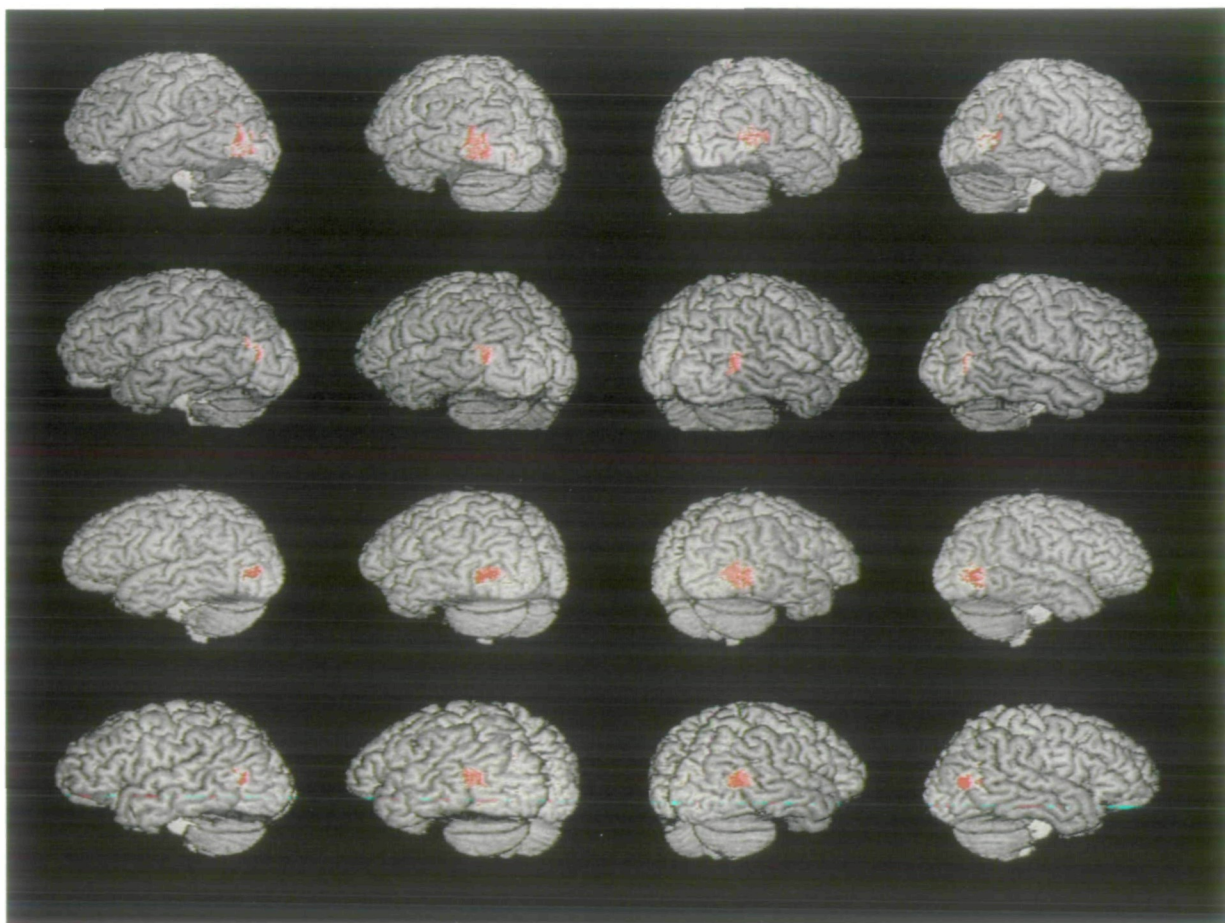


Figure 6. The cerebral hemispheres from four subjects, showing each V5 area as defined by the PET activation experiments, superimposed on the individual's own MR image. Each subject occupies a row; the first row is the subject shown in Figure 5. The images were derived from slice data such as that presented in Figure 5, but are now displayed as surface-rendered objects viewed at rotations of 90° and 50° from the occipital pole, to allow the patterns of sulci and gyri to be seen. In each subject the PET SPM(t) image was edited to leave only V5. The statistical threshold was lowered so that the PET image was contiguous with the cortical surface of the MRI after the PET and MR images were coregistered and superimposed, so that the process of surface rendering (to a depth of some eight pixels) does not falsely locate the site of V5 in terms of surface features. The PET activation sites were rendered as red areas on the final images.

of spatial filtering (which reduces the peaks of rCBF change) and the variation in the location of V5 across individuals such that the anatomical transformation into Talairach coordinates fails to superimpose the foci from different individuals onto one another. With a set filter size, as more subjects are added to a group, the average increase recorded in rCBF will tend to decline (Raichle et al., 1991), at least down to a certain point.

Group versus Individual Studies

We consider here the relative merits of studying groups and single individuals. Each type of study provides important information but has problems attached to it. The necessity for using groups in PET experiments arose from the simple problem that, at the permitted doses of administered radiation, the signal-to-noise ratio was generally too low to inspire confidence in results obtained from single subjects. Because they increase the signal-to-noise ratio, grouped data are more reliable. They extract the most significant and commonplace activation sites even if they sacrifice the individual patterns of activation; some of the latter, although divergent from the mean, may never-

theless contain important lessons. In addition, grouped results in reference to standard stereotaxic coordinates allow an easier comparison of results obtained with different paradigms, in different laboratories, and with different groups of subjects. The method has its drawbacks, however, especially in relating the site of activation to the anatomy of the cerebral cortex. In addition, the method is awkward to use when single patients, manifesting a rare condition, are the subject of study. These drawbacks can be compensated for by the use of more advanced techniques, such as we have used, which allow the repeated scanning of single subjects at the same dose of radiation and give results with greater statistical confidence. Because single subjects are used, the PET images can be coregistered with MR images. The site of activation can thus be directly related to the anatomy of the cerebral cortex. Nevertheless, the study of single subjects inspires greater confidence when the results obtained from it are, so to speak, validated by group results that show that a similar area is active when the same task is used in a group of subjects. For example, in this study we used the position of V5 as defined in the analysis of the group of 12 subjects

as the basis on which to search for V5 in each individual. We thus tend to use both approaches simultaneously, preferring the former for the screening of the cerebral areas involved in the execution of a task and the latter for a more detailed study of the area in relation to the anatomy of the brain.

PET studies often use small groups of about six to eight subjects. This small size, along with the individual biological variation, the characteristics of low-pass filtering and the statistical methods, will all combine to make the reporting of results in terms of standard stereotaxic coordinates uncertain. The subgroup analysis performed in this study showed that intersubject variability alone can allow a reported activation site to vary by close to the width of a gyrus. Put more simply, even standardized coordinates are uncertain. Even if they were certain, relocating them onto the single brain used in the Talairach and Tournoux system will only be valid as far as that brain, measured in the postmortem and fixed state, reflects the actual anatomy of the individuals that made up the PET study group.

V5 Areas in Individuals, Coregistered with MRI Scans

Having identified the location of area V5 on the SPM{t} maps for each individual subject after stereotaxic normalization, we used the same statistical approach to find the same areas for each subject, but this time without anatomically transforming the PET images. In other words, the locations were now expressed in the unique reference framework of each subject's own brain, and not in terms of a standard reference framework. It was then possible to coregister the individual PET results with the corresponding MR images, which in turn allowed us to locate areas such as V5 with respect to the more detailed anatomy of the brain in terms of sulci and gyri. In gyrencephalic brains, a focus of activation might fall on the surface of the cerebral cortex, or it might be buried deep within a sulcus and thus not be visible on the surface. Because of this, one needs both two- and three-dimensional reconstructions for the process of anatomical localization (Figs. 5, 6). Two-dimensional reconstructions are vital for identifying structures lying within sulci (as V5 may be), while three-dimensional reconstructions are instrumental in identifying the detailed surface configuration of the brain in terms of sulci and gyri, and the relationship of an activated area to them. Hence, an added advantage of using MR images with voxel dimensions less than 1.5 mm was the ability to make such three-dimensional reconstructions. The latter helped us to identify the pattern of sulci and gyri in the occipital lobes of all our subjects (24 hemispheres) and thus make a statement about the relationship of area V5 to the sulcal and gyral pattern of the occipital lobe of the human brain.

The Pattern of Gyri and Sulci in the Occipital Lobe of the Human Brain

Topographical-functional relationships in the human cerebral cortex have been known to exist for many

years. Chief among these is the relationship of the primary visual cortex to the calcarine sulcus of the occipital lobe (Henschen, 1893; Flechsig, 1905). It therefore seemed plausible that such relationships might be found elsewhere in the occipital lobe. There is, however, a great deal of variability in the pattern of fissuration of the occipital cortex. Perhaps for this very reason, the literature contains a scanty and unsatisfactory description of the gyral anatomy of the lateral occipital lobe. There are nevertheless some sulcal patterns that seem to bear a more or less consistent relationship to the position of human V5. We therefore provide a brief description of the occipital lobe with the hope of specifying the position of human V5 with as little ambiguity as possible.

Most descriptions of the lateral occipital lobe divide it into gyri. Some consider that there are three gyri—the upper, middle, and lower occipital gyri (Talairach and Tournoux, 1988); others divide it into just two, the lateral and superior gyri, while admitting that the lateral gyrus may have further subdivisions (Cunningham, 1902; Toldt, 1908). These descriptions rely on a horizontally oriented sulcus, the *lateral occipital*, of which there are sometimes two lying parallel with each other (Ono et al., 1990). By contrast, the International Anatomical Nomenclature Committee (1989) recognizes only two sulci, the *transverse occipital* and the variable *lunate*, both of which are angled dorsoventrally and hence do not subdivide the occipital lobe into gyri stacked upon one another. We found that the most useful landmark for identifying the position of area V5 is the posterior continuation of the *inferior temporal sulcus*. This is present in the great majority of hemispheres, though it adopts a variety of forms. Normally it runs dorsoventrally at the border between the temporal and occipital lobes; it is so identified by Cunningham (1902), who refers to it as the *ascending limb of the inferior temporal sulcus*, and by Toldt (1908), who calls it the *anterior occipital sulcus*. As the latter term has also been applied to other nearby sulci (Ono et al., 1990), we prefer the former term, which we abbreviate to ALITS. V5 lies at the junction of ALITS with the *lateral occipital sulcus*. Where the two do not actually intersect, as commonly happens, V5 is to be found near their interpolated meeting point (e.g., Fig. 6, first row, right). The site of activation may fall within the sulcus, at least in part (Fig. 5). In fact, the *inferior temporal* is a highly interrupted sulcus that is not always easily identified. In some hemispheres its posterior continuation is better identified as a separate, transversely oriented sulcus, often extending over the inferolateral margin of the occipital lobe (see Fig 7). Again, V5 is situated posterior to this sulcus, near its dorsal termination (e.g., Fig. 6, first and third rows, left; Fig. 8).

One or the other of these patterns sufficed to describe the location of V5 in 16 of our 24 hemispheres. In the remainder, the patterns were suggestive but less clear cut. On the basis of its dense myelination, Clarke and Miklossy (1990) located an area that they considered to be area V5 in a similar region. In the

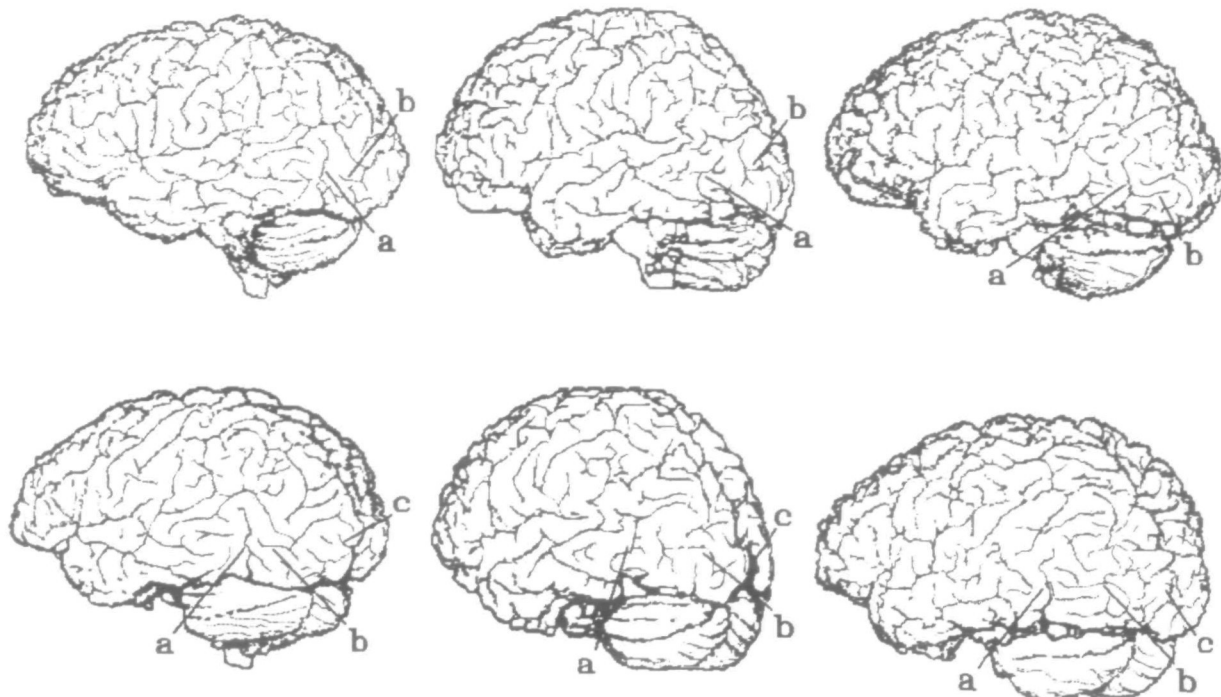


Figure 7. Line diagrams of the left hemispheres of three subjects to show variation in the surface anatomy of the occipital lobe. The upper row contains lateral views, while the lower row has views with a 30° rotation. *a*, ascending limb of inferior temporal sulcus, also known as anterior occipital sulcus; *b*, lateral occipital sulcus; *c*, tip of calcarine sulcus.

sketch of the brain they provide, the inferior temporal sulcus runs more or less continuously into the lateral occipital, and lacks an obvious ascending limb. Despite this somewhat different sulcal anatomy, the lo-

cation they illustrate is quite consistent with the location of area V5 derived from our studies.

Not the least interesting feature of a location for V5 just posterior to ALITS is that it coincides almost exactly with Flechsig's *Feld 16* in what he calls the *gyrus subangularis* (Flechsig, 1920) (see Fig. 8). This *Feld 16*, which is classed among the *Prämature Rindenfelder*, thus belongs to cortex which is myelinated at birth, though Flechsig states that it is not as heavily myelinated at birth as the other areas comprising this group, among which he numbers the calcarine cortex (area V1). According to Flechsig, the myelination spreads postnatally to include *Feld 27*, lying just anterior. If area V5 is well demarcated at birth, by virtue of its early myelogenesis, it is not inconceivable that herein lies the link between function and gyral morphology—the arrival of afferents to this zone perhaps promoting an infolding of the cortical sheet. We note in the same context that Bailey and von Bonin (1951, their Fig. 7) show the "anterior occipital sulcus" already beginning to form in the 30 week embryo.

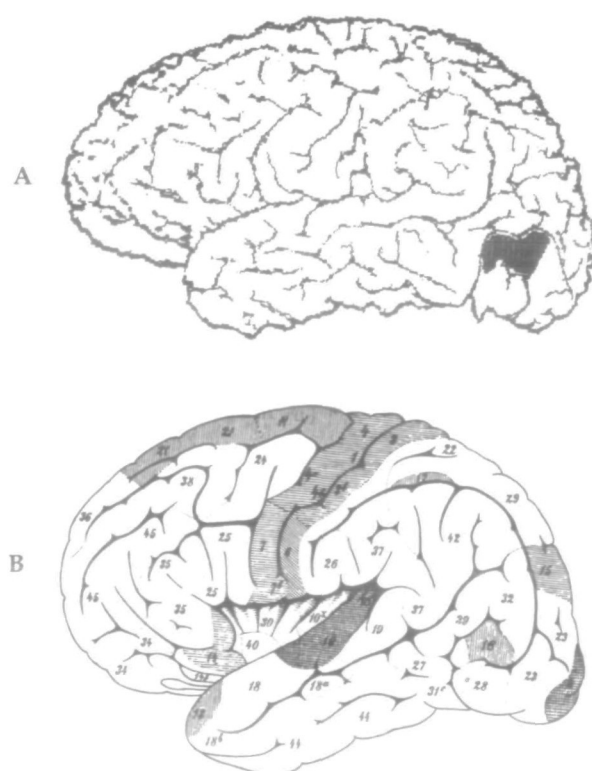


Figure 8. *A*, The position of human area V5 in an individual brain, as determined in this study. *B*, Flechsig's diagram of the myeloarchitecture of the human brain. Compare the position of *Feld 16* with that of V5 in *A*.

Other Areas

We suggest provisionally that the areas of activation found bilaterally in the cuneus and the lingual gyri are part of one functional area that corresponds to area V3 in the monkey. On topographical grounds, it is reasonable to expect V3 to lie juxtaposed with the V1/V2 complex, both from the anatomical findings in macaque and from the recent arguments based on lesion studies in man (Horton and Hoyt, 1991). Furthermore, in all subjects scanned high enough, there was a ribbon-like area of activation in parietal cortex, extending forward from the parieto-occipital fissure.

This is Brodmann's area 7, a region that in the monkey at least is known to receive input from V5, and other prestriate areas (Maunsell and Van Essen, 1983; Ungerleider and Desimone, 1986; Cavada and Goldman-Rakic, 1989; Andersen et al., 1990; Zeki, 1990). It is of interest that a previous study, intended to chart the retinotopic organization of striate cortex, also revealed a somewhat similar distribution of activated regions in prestriate cortex—although V5 was not specifically identified (Fox et al., 1987). In fact, that study employed an alternating checkerboard stimulus. The latter lacks coherent motion but is otherwise similar to ours in its spatiotemporal properties.

In summary, we show that methodological improvements in PET scanning, and the coregistration of PET and MR images, allow the organization of visual pathways to be studied in single subjects. This approach complements studies in groups of subjects that are essential to an identification of the common cortical areas related to particular functions, especially when the blood flow changes elicited are small. Studies in individuals will be invaluable and of crucial importance in those informative but rare patients with selective loss of cortical function.

Notes

We are most grateful to all our volunteers, who provided so much time and effort for this study. We thank Professor G M. Bydder, Dr. W. Curati, Professor I. R. Young, Mrs. S. White, and Miss K. Williams of the NMR Unit at the Royal Post-graduate Medical School, Hammersmith Hospital, for their encouragement and their help in performing the MRI scans. From the MRC Cyclotron Unit we thank Mr. G. Lewington, Ms. C. Taylor, and Ms. A. Williams for carrying out the PET scans, Dr. J. Clarke and the radiochemistry section for developing the water generator, and Dr. T. Jones, Mr. D. L. Bailey, Dr. T. J. Spinks, and Ms. S. Grootoont for the introduction of three-dimensional PET scanning. We also thank Mr. J. Romaya, from the Department of Anatomy, University College, London, for developing the computer displays of visual stimuli.

Correspondence should be addressed to S. Zeki, Department of Anatomy, University College London, London WC1E 6BT, UK, or to R. S. J. Frackowiak, MRC Cyclotron Unit, Hammersmith Hospital, London W12 0HS, UK.

References

- Andersen RA, Asanuma C, Essick G, Siegel RM (1990) Cortico-cortical connections of anatomically defined subdivisions within the inferior parietal lobule. *J Comp Neurol* 296:65–113.
- Bailey DL, Jones T, Spinks TJ (1991a) A method for measuring the absolute sensitivity of positron emission tomographic scanners. *Eur J Nucl Med* 18:374–379.
- Bailey DL, Jones T, Spinks TJ, Gilardi M-C, Townsend DW (1991b) Noise equivalent count measurements in a neuro-PET scanner with retractable septa. *IEEE Trans Med Imaging* 10:256–260.
- Bailey P, von Bonin G (1951) The isocortex of man. Urbana: University of Illinois.
- Belliveau JW, Kennedy DN, McKinstry RC, Buchbinder BR, Weisskoff RM, Cohen MS, Vevea JM, Brady TJ, Rosen BR (1991) Functional mapping of the human visual cortex by magnetic resonance imaging. *Science* 254:716–719.
- Cavada C, Goldman-Rakic P (1989) Posterior parietal cortex in rhesus monkey: I. Parcellation of areas based on distinctive limbic and sensory corticocortical connections. *J Comp Neurol* 287:393–421.
- Clarke S, Miklossy J (1990) Occipital cortex in man: organization of callosal connections, related myelo- and cytoarchitecture, and putative boundaries of functional visual areas. *J Comp Neurol* 298:188–214.
- Cragg BG (1969) The topography of the afferent projections in the circumstriate visual cortex of the monkey studied by the Nauta method. *Vision Res* 9:733–747.
- Cunningham DJ (1902) Text-book of anatomy. London: Pentland.
- Desimone R, Ungerleider LG (1986) Multiple visual areas in the caudal superior temporal sulcus of the macaque. *J Comp Neurol* 248:164–189.
- Evans AC, Marrett S, Torrerosco J, Ku S, Collins L (1991) MRI-PET correlation in three dimensions using a volume-of-interest (VOI) atlas. *J Cereb Blood Flow Metab* 11:A69–A78.
- Flechsig P (1905) Gehirnphysiologie und Willenstheorie. Paper presented at Fifth International Psychology Congress, Rome. Reprinted in: Some papers on the cerebral cortex (von Bonin G, trans), pp 181–200. Springfield, IL: Thomas, 1960.
- Flechsig P (1920) Anatomie des menschlichen Gehirns und Rückenmarks. Leipzig: Thieme.
- Fox PT, Mintun MA (1989) Noninvasive functional brain mapping by change-distribution analysis of averaged PET images of $H_2^{15}O$ tissue activity. *J Nucl Med* 30:141–149.
- Fox PT, Miezin FM, Allman JM, Van Essen DC, Raichle ME (1987) Retinotopic organisation of human visual cortex mapped with positron emission tomography. *J Neurosci* 7:913–922.
- Friston KJ, Frackowiak RSJ (1991) Imaging functional anatomy. In: Brain work and mental activity. Quantitative studies with radioactive tracers (Lassen NA, Ingvar DH, Raichle ME, Friberg L, eds), pp 267–279. Copenhagen: Munksgaard.
- Friston KJ, Frith CD, Liddle PF, Dolan RJ, Lammertsma AA, Frackowiak RSJ (1990) The relationship between global and local changes in PET scans. *J Cereb Blood Flow Metab* 10:458–466.
- Friston KJ, Frith CD, Liddle PF, Frackowiak RSJ (1991a) Plastic transformation of PET images. *J Comput Assist Tomogr* 15:634–639.
- Friston KJ, Frith CD, Liddle PF, Frackowiak RSJ (1991b) Comparing functional (PET) images: the assessment of significant change. *J Cereb Blood Flow Metab* 11:690–699.
- Grafton ST, Mazziotta JC, Woods RP, Phelps ME (1992) Human functional anatomy of visually guided finger movements. *Brain* 115:565–587.
- Henschen SE (1893) On the visual path and centre. *Brain* 16:170–180.
- Horton JC, Hoyt WF (1991) Quadrantic visual field defects: a hallmark of lesions in extrastriate cortex (V2/V3). *Brain* 114:1703–1718.
- International Anatomical Nomenclature Committee (1989) Nomina anatomica, 6th ed. London: Churchill Livingstone.
- Kaplan E, Shapley RM (1982) X and Y cells in the lateral geniculate nucleus of macaque monkeys. *J Physiol (Lond)* 330:125–143.
- Maunsell JH, Van Essen DC (1983) The connections of the middle temporal visual area (MT) and their relationship to a cortical hierarchy in the macaque monkey. *J Neurosci* 3:2563–2586.
- Mazziotta JC, Huang SC, Phelps ME, Carson RE, MacDonald NS, Mahoney K (1985) A non-invasive positron computed tomography technique using oxygen-15 labeled water for the evaluation of neurobehavioral task batteries. *J Cereb Blood Flow Metab* 5:70–78.
- Miezin FM, Fox PT, Raichle ME, Allman JM (1987) Localized responses to low contrast moving random dot patterns in human visual cortex monitored with positron emission tomography. *Soc Neurosci Abstr* 13:631.
- Oldfield RC (1971) The assessment and analysis of hand-

- edness: the Edinburgh inventory. *Neuropsychologia* 9:97–113.
- Ono M, Kubik S, Abernathey CD (1990) *Atlas of the cerebral sulci*. Stuttgart: Thieme.
- Pelizzari CA, Chen GT, Spelbring DR, Weichselbaum RR, Chen CT (1989) Accurate three-dimensional registration of CT, PET, and/or MR images of the brain. *J Comput Assist Tomogr* 13:20–26.
- Raichle ME (1987) Circulatory and metabolic correlates of brain function in normal humans. In: *Handbook of physiology: the nervous system*, Vol V (Plum F, ed), pp 643–674. New York: American Physiology Society–Oxford UP.
- Raichle ME, Mintun MA, Shertz LD, Fusselman MJ, Miezen F (1991) The influence of anatomical variability on the functional brain mapping with PET: a study of intrasubject versus intersubject averaging. *J Cereb Blood Flow Metab* 11:S364.
- Schachter SC, Ransil BJ, Geschwind N (1987) Associations of handedness with hair color and learning disabilities. *Neuropsychologia* 25:269–276.
- Spinks TJ, Jones T, Bailey DL, Townsend DW, Grootoornk S, Bloomfield PM, Gilardi M-C, Casey ME, Sipe B, Reed J (1992) Physical performance of a positron tomograph for brain imaging with retractable septa. *Phys Med Biol* 37:1637–1655.
- Talairach J, Tournoux P (1988) *Co-planar stereotaxic atlas of the human brain*. Stuttgart: Thieme.
- Talairach J, Szikla G, Tournoux P, Prossalantis A, Bordas-Ferrer M, Covello L, Iacob M, Mempel E (1967) *Atlas of stereotaxic anatomy of the telencephalon*. Paris: Masson.
- Tanaka K, Hikosaka K, Saito H, Yukie M, Fukada Y, Iwai E (1986) Analysis of local and wide-field movements in the superior temporal visual areas of the macaque monkey. *J Neurosci* 6:134–144.
- Toldt C (1908) *Anatomischer Atlas für Studierende und Ärzte*. Berlin: Urban and Schwarzenberg.
- Tootell RBH, Hamilton SL, Switkes E (1988) Functional anatomy of macaque striate cortex IV: Contrast and magnano-parvo streams. *J Neurosci* 8:1594–1609.
- Townsend DW, Geissbuhler A, Defrise M, Hoffman EJ, Spinks TJ, Bailey DL, Gilardi M-C, Jones T (1991) Fully three-dimensional reconstruction for a PET camera with retractable septa. *IEEE Trans Med Imaging* 10:505–512.
- Ungerleider LG, Desimone R (1986) Cortical connections of visual area MT in the macaque. *J Comp Neurol* 248:190–222.
- Woods RP, Cherry SR, Mazziotta JC (1992) A rapid automated algorithm for accurately aligning and reslicing positron emission tomography images. *J Comput Assist Tomogr* 16:620–633.
- Wurtz RH, Yamasaki DS, Duffy CJ, Roy J-P (1990) Functional specialization for visual motion processing in primate cerebral cortex. *Cold Spring Harbor Symp Quant Biol* 55:717–727.
- Zeki SM (1969) Representation of central visual fields in prestriate cortex of monkey. *Brain Res* 14:271–291.
- Zeki SM (1974) Functional organization of a visual area in the posterior bank of the superior temporal sulcus of the rhesus monkey. *J Physiol (Lond)* 236:549–573.
- Zeki SM (1977a) Colour coding in the superior temporal sulcus of the rhesus monkey visual cortex. *Proc R Soc Lond [Biol]* 197:195–223.
- Zeki SM (1977b) Simultaneous anatomical demonstration of the vertical and horizontal meridians in areas V2 and V3 of rhesus monkey visual cortex. *Proc R Soc Lond [Biol]* 195:517–523.
- Zeki SM (1978) The third visual complex of rhesus monkey prestriate cortex. *J Physiol (Lond)* 277:245–272.
- Zeki S (1980) The response of cells in the anterior bank of the superior temporal sulcus in macaque monkeys. *J Physiol (Lond)* 308:85P.
- Zeki S (1990) *The motion pathways of the visual cortex*. In: *Vision, coding and efficiency* (Blakemore C, ed), pp 321–345. Cambridge: Cambridge UP.
- Zeki S, Watson JDG, Lueck CJ, Friston KJ, Kennard C, Frackowiak RSJ (1991) A direct demonstration of functional specialization in human visual cortex. *J Neurosci* 11:641–649.
- Zihl J, von Cramon D, Mai N (1983) Selective disturbance of movement vision after bilateral brain damage. *Brain* 106:313–340.
- Zihl J, von Cramon D, Mai D, Schmid Ch (1991) Disturbance of movement vision after bilateral posterior brain damage. Further evidence and follow up observations. *Brain* 114:2235–2252.